INTERNATIONAL JOURNAL OF
NUMERICAL ANALYSIS AND MODELING
Volume 10, Number 4, Pages 775–794

A NEW ENERGY-CONSERVED S-FDTD SCHEME FOR MAXWELL'S EQUATIONS IN METAMATERIALS

WANSHAN LI, DONG LIANG, AND YANPING LIN

Abstract. In this paper, we develop a new energy-conserved S-FDTD scheme for the Maxwell's equations in metamaterials. We first derive out the new property of energy conservation of the governing equations in metamaterials, and then propose the energy-conserved S-FDTD scheme for solving the problems based on the staggered grids. We prove that the proposed scheme is energy-conserved in the discrete form and unconditionally stable. Based on the energy method, we further prove that the scheme for the Maxwell's equations in metamaterials is first order in time and second order in space. Numerical experiments are carried out to confirm the energy conservation and the convergence rates of the scheme. Moreover, numerical examples are also taken to show the propagation features of electromagnetic waves in the DNG metamaterials.

Key words. Maxwell's equations, metamaterials, energy-conserved, splitting, FDTD, convergence

1. Introduction

Metamaterials are defined as artificial engineered materials exhibiting unique or unusual properties that cannot be found in natural materials at the frequencies of interest. Metamaterials have been used in many applications, that allow going beyond some limitations encountered when using natural materials, such as microwave and optical components, interconnects for wireless telecommunications, radar and defense, nanolithography and medical imaging at sub-wavelength resolution, construction of perfect lens and so on (see, [1, 27, 25, 26, 5, 9]).

Many kinds of metamaterials, such as double-negative (DNG) materials, negative index materials (NIM), left-handed materials (LHM) and back-ward (BW) media, are constructed, developed and studied ([4, 6, 21, 31]). For examples, DNG materials mean that the permittivity and permeability of the materials are both negative at the frequencies of interest; the NIM materials refer to the fact that the materials with simultaneously negative real parts of permittivity and permeability exhibit a negative real part of the refraction index, leading to anomalous refraction properties. In these kinds of metamaterials, the periodicity is much smaller than the wavelength of the impinging electromagnetic wave. Hence they are useful and customary continuous materials.

Some study of numerical simulations for Maxwell's equations in metamaterials have carried out (see, for example, [28]). Such simulations are exclusively based on the finite-difference time-domain (FDTD) methods. Due to the constraint (i.e. the CFL stability condition) of the FDTD methods, it leads to impractical computational costs and memory requirement in broadband applications in high dimensional and large domains. Therefore, there is an urgent call for developing more efficient and reliable numerical methods for metamaterial simulations. To overcome the CFL restriction of the FDTD schemes for the standard Maxwell's equations, some

Received by the editors January 29, 2013 and, in revised form, February 17, 2013.
2000 *Mathematics Subject Classification.* 65M10, 65M15, 65N10, 65N15.
The work was supported partially by NSERC (Canada) and GRF of HKSAR(PolyU 5010/12P).
Corresponding author: Dong Liang; Email: *dliang@mathstat.yorku.ca*.

ADI-FDTD ([22, 29, 8, 12]), S-FDTD ([7]) and EC-S-FDTD ([2]) schemes were developed for the standard Maxwell's equations. But, there are few results of the ADI-FDTD, S-FDTD schemes for solving the electromagnetic problems in metamaterials. On the theoretical analysis aspect, for problems of metamatrials, some work of finite element methods (FEM) and the discontinuous Galerkin methods (DG) were analayzed ([10, 11, 13, 14, 15, 16, 17, 18, 19, 20]). However, there is no theoretical analysis work of the FDTD, ADI-FDTD, S-FDTD schemes for the Maxwell's equations that metamaterials are involved.

In this paper, we develop the energy-conserved S-FDTD scheme for the Maxwell's equations in metamaterials by focussing on preserving physical property of energy conservation. We first derive out the new property of energy conservation of the Maxwell's equations in metamaterials. We then propose an energy-conserved splitting FDTD scheme (EC-S-FDTD) for solving the problems that metamaterials are involved. We prove that the proposed EC-S-FDTD scheme satisfies the energy-conserved identity in the discrete form and the scheme is unconditionally stable. We further analyze the error estimates of the scheme and prove strictly that the scheme is of first-order convergence in time step and second-order convergence in spatial step. In numerical experiments, we show numerically the energy conservation property and the convergence rates of the EC-S-FDTD scheme and also simulate numerically the physical phenomena of electromagnetic wave propagation in the NDG metamaterials ([24, 30, 23]). Numerical results confirm our theoretical results.

The paper is organized as follows. Section 2 introduces the Maxwell's equations in metamaterials and derives the new energy conservation identity of electromagnetic fields in metamaterials. A new energy-conserved S-FDTD scheme is proposed in Section 3. We prove the discrete energy conservation, the unconditional stability of the proposed scheme in Section 4 and analyze the convergence of the scheme in Section 5. Numerical experiments are presented in Section 6. Finally, conclusions are addressed in Section 7.

2. Maxwell's equations in metamaterials

We consider the Maxwell's equations in the DNG metamaterials with the lossy Drude model. The general Maxwell's equations are

$$\nabla \times \mathbf{E} = -\frac{\partial \mathbf{B}}{\partial t}, \tag{1}$$

$$\nabla \times \mathbf{H} = \frac{\partial \mathbf{D}}{\partial t}, \tag{2}$$

where $\mathbf{E}(\mathbf{x}, t)$ and $\mathbf{H}(\mathbf{x}, t)$ are the electric and magnetic fields, $\mathbf{D}(\mathbf{x}, t)$ and $\mathbf{B}(\mathbf{x}, t)$ are the corresponding electric and magnetic flux densities. $\mathbf{D}$ and $\mathbf{B}$ are related to $\mathbf{E}$ and $\mathbf{H}$ through the constitutive relations:

$$\mathbf{D} = \epsilon_0 \mathbf{E} + \mathbf{P} \equiv \epsilon \mathbf{E}, \qquad \mathbf{B} = \mu_0 \mathbf{H} + \mathbf{M} \equiv \mu \mathbf{H}, \tag{3}$$

where ϵ_0 is the vacuum permittivity, μ_0 is the vacuum permeability, and $\mathbf{P}$ and $\mathbf{M}$ are the induced electric and magnetic polarizations, respectively. We use the lossy Drude polarization and magnetization models [3, 32] to describe the DNG metamaterials. In the frequency domain, the permittivity and permeability are described as:

$$\epsilon(\omega) = \epsilon_0\big(1 - \frac{\omega_{pe}^2}{\omega(\omega + i\Gamma_e)}\big), \quad \mu(\omega) = \mu_0\big(1 - \frac{\omega_{pm}^2}{\omega(\omega + i\Gamma_m)}\big), \tag{4}$$

where ω_{pe} and ω_{pm} are the significant physical parameters representing the character of plasma, i.e., electric and magnetic plasma resonance frequencies respectively, ω is the angular frequency of the incident wave, and Γ_e and Γ_m are the electric and magnetic damping frequencies, respectively.

The corresponding time-domain equations for the polarization $\mathbf{P}$ and the magnetization $\mathbf{M}$ are:

$$\begin{aligned} \frac{\partial^2 \mathbf{P}}{\partial t^2} + \Gamma_e \frac{\partial \mathbf{P}}{\partial t} &= \epsilon_0 \omega_{pe}^2 \mathbf{E}, \\ \frac{\partial^2 \mathbf{M}}{\partial t^2} + \Gamma_m \frac{\partial \mathbf{M}}{\partial t} &= \mu_0 \omega_{pm}^2 \mathbf{H}. \end{aligned} \tag{5}$$

Let the induced electric and magnetic currents be

$$\mathbf{J} = \frac{\partial \mathbf{P}}{\partial t}, \qquad \mathbf{K} = \frac{\partial \mathbf{M}}{\partial t}. \tag{6}$$

Thus, the Maxwell's equations modeling the electromagnetic fields in the DNG metamaterial medium described as:

$$\epsilon_0 \frac{\partial \mathbf{E}}{\partial t} = \nabla \times \mathbf{H} - \mathbf{J}, \tag{7}$$

$$\mu_0 \frac{\partial \mathbf{H}}{\partial t} = -\nabla \times \mathbf{E} - \mathbf{K}, \tag{8}$$

$$\frac{\partial \mathbf{J}}{\partial t} + \Gamma_e \mathbf{J} = \epsilon_0 \omega_{pe}^2 \mathbf{E}, \tag{9}$$

$$\frac{\partial \mathbf{K}}{\partial t} + \Gamma_m \mathbf{K} = \mu_0 \omega_{pm}^2 \mathbf{H}. \tag{10}$$

Assume that the boundary of Ω is perfectly conducting, i.e.,

$$\mathbf{n} \times \mathbf{E} = \mathbf{0}, \quad or \quad \mathbf{n} \times \mathbf{H} = \mathbf{0}, on\ \partial\Omega, \tag{11}$$

where $\mathbf{n}$ is the unit outward normal to $\partial\Omega$. The initial conditions are

$$\mathbf{E}(x,y,t) = \mathbf{E_0}(x,y,t), \quad \mathbf{H}(x,y,t) = \mathbf{H_0}(x,y,t), \tag{12}$$

$$\mathbf{J}(x,y,t) = \mathbf{J_0}(x,y,t), \quad \mathbf{K}(x,y,t) = \mathbf{K_0}(x,y,t). \tag{13}$$

We now derive the energy conservation of the Maxwell's equations (7)-(13) in metamaterials and without sources. From (7) -(8) and (6), we get

$$\int_0^t \Big\{ \Big(\epsilon_0 \frac{\partial \mathbf{E}}{\partial t}, \mathbf{E}\Big) + \Big(\mu_0 \frac{\partial \mathbf{H}}{\partial t}, \mathbf{H}\Big) + \Big(\mathbf{J}, \mathbf{E}\Big) + \Big(\mathbf{K}, \mathbf{H}\Big) \Big\} d\tau = -\int_0^t \int_{\partial\Omega} (\mathbf{E} \times \mathbf{H}) \cdot \mathbf{n} ds d\tau, \tag{14}$$

where $(\cdot,\cdot)$ denotes the $L^2(\Omega)$ inner product. (14) follows the Poynting theory. The first and third terms on the left side of (14) represent the increasing rates of the electric field energy and the polarization power respectively, while the terms $(\mu_0 \frac{\partial \mathbf{H}}{\partial t}, \mathbf{H})$ and $(\mathbf{K}, \mathbf{H})$ are the increasing rates of the magnetic field energy and the magnetization power respectively. With equations (9), (10) and the PEC boundary condition (11), it holds that

$$\begin{aligned} &\frac{1}{2} \frac{d(\epsilon_0 \mathbf{E}, \mathbf{E})}{dt} + \frac{1}{2} \frac{d(\mu_0 \mathbf{H}, \mathbf{H})}{dt} + \frac{1}{2\epsilon_0 \omega_{pe}^2} \frac{d(\mathbf{J}, \mathbf{J})}{dt} + \frac{1}{2\mu_0 \omega_{pm}^2} \frac{d(\mathbf{K}, \mathbf{K})}{dt} \\ &\qquad + \frac{\Gamma_e}{\epsilon_0 \omega_{pe}^2} (\mathbf{J}, \mathbf{J}) + \frac{\Gamma_m}{\mu_0 \omega_{pm}^2} (\mathbf{K}, \mathbf{K}) = 0. \end{aligned} \tag{15}$$

Let $W(t)$ be the electromagnetic energy in the case of metamaterials. Integrating with respect to t for both sides of (15), we finally have that

$$
\begin{aligned}
W(t) \equiv & \epsilon_0||\mathbf{E}(t)||^2 + \mu_0||\mathbf{H}(t)||^2 + \frac{1}{\epsilon_0\omega_{pe}^2}||\mathbf{J}(t)||^2 + \frac{1}{\mu_0\omega_{pm}^2}||\mathbf{K}(t)||^2 \\
& + \frac{2\Gamma_e}{\epsilon_0\omega_{pe}^2}\int_0^t ||\mathbf{J}(\tau)||^2 d\tau + \frac{2\Gamma_m}{\mu_0\omega_{pm}^2}\int_0^t ||\mathbf{K}(\tau)||^2 d\tau \\
= & \epsilon_0||\mathbf{E}(0)||^2 + \mu_0||\mathbf{H}(0)||^2 + \frac{1}{\epsilon_0\omega_{pe}^2}||\mathbf{J}(0)||^2 + \frac{1}{\mu_0\omega_{pm}^2}||\mathbf{K}(0)||^2 \equiv W(0),
\end{aligned} \tag{16}
$$

which indicates that the electromagnetic energy is conserved. The above analysis leads to a new energy conservation of Maxwell's equations in metamaterials.

Theorem 1. *(Energy conservation) For Maxwell's equations (7)-(13) in metamaterials, the electromagnetic energy (16) is conserved.*

Remark 1: From (16), it is clear that in metamaterials with no sources, the electromagnetic energy $W(t)$ is conserved. This physical invariance of energy is the most important feature on the prorogation of electromagnetic wave. It thus is an important issue to construct numerical schemes to preserve energy conservation for solving the electromganetic system of PDEs in metamaterials. In this study, we will further propose an efficient energy-conserved splitting FDTD scheme to the Maxwell's system in metamaterials that preserves the new important identity of energy conservation (16) in the discrete form.

3. The energy-conserved S-FDTD scheme

For simplicity, we consider the two-dimensional problems in metamaterials. The domain is $\Omega = [a,b] \times [c,d]$, $t \in [0,T]$. The Maxwell's equations in two dimensional metamaterials are as follows

$$\epsilon_0 \frac{\partial E_z}{\partial t} = \frac{\partial H_y}{\partial x} - \frac{\partial H_x}{\partial y} - J_z, \tag{17}$$

$$\mu_0 \frac{\partial H_x}{\partial t} = -\frac{\partial E_z}{\partial y} - K_x, \tag{18}$$

$$\mu_0 \frac{\partial H_y}{\partial t} = \frac{\partial E_z}{\partial x} - K_y, \tag{19}$$

$$\frac{\partial J_z}{\partial t} + \Gamma_e J_z = \epsilon_0 \omega_{pe}^2 E_z, \tag{20}$$

$$\frac{\partial K_x}{\partial t} + \Gamma_m K_x = \mu_0 \omega_{pm}^2 H_x, \tag{21}$$

$$\frac{\partial K_y}{\partial t} + \Gamma_m K_y = \mu_0 \omega_{pm}^2 H_y, \tag{22}$$

and the initial conditions are

$$E_z(x,y,t) = E_0(x,y,t), \quad \mathbf{H}(x,y,t) = \mathbf{H_0}(x,y,t), \tag{23}$$

$$J_z(x,y,t) = J_0(x,y,t), \quad \mathbf{K}(x,y,t) = \mathbf{K_0}(x,y,t), \tag{24}$$

the PEC boundary conditions are

$$E_z(a,y,t) = E_z(b,y,t) = E_z(x,c,t) = E_z(x,d,t) = 0. \tag{25}$$

First, we take the following partitions. Let I, J, and N be positive integers. Let $\Delta x = (b-a)/I$ and $\Delta y = (d-c)/J$ be the spacial step sizes of $x-$direction and $y-$direction respectively, and $\Delta t = T/N$ be the time step length. We adopt the Yee's staggered grids. For $i = 0, 1, \cdots, I$, $j = 0, 1, \cdots, J$ and $n = 0, 1, \cdots, N$, define

$x_i = a + i\Delta x$, $y_j = c + j\Delta y$, $t_n = n\Delta t$, $x_{i+\frac{1}{2}} = x_i + \frac{1}{2}\Delta x$, $y_{j+\frac{1}{2}} = y_j + \frac{1}{2}\Delta y$ and $t_{n+\frac{1}{2}} = t_n + \frac{1}{2}\Delta t$. The spacial mesh indices are $(i, j+\frac{1}{2})$ for H_x and K_x, $(i+\frac{1}{2}, j)$ for H_y and K_y, and (i, j) for E_z and J_z. The grid function $U^n_{\alpha,\beta}$ is defined on the staggered grid where $\alpha = i$ or $i+\frac{1}{2}$ and $\beta = j$ or $j+\frac{1}{2}$. The spatial difference operators $\delta_x U$, $\delta_y U$ and $\delta_u\delta_v U$ are defined as:

$$\begin{aligned}\delta_t U^n_{\alpha,\beta} &= \frac{U^{n+\frac{1}{2}}_{\alpha,\beta} - U^{n-\frac{1}{2}}_{\alpha,\beta}}{\Delta t},\ \delta_x U^n_{\alpha,\beta} = \frac{U^n_{\alpha+\frac{1}{2},\beta} - U^n_{\alpha-\frac{1}{2},\beta}}{\Delta x},\\ \delta_y U^n_{\alpha,\beta} &= \frac{U^n_{\alpha,\beta+\frac{1}{2}} - U^n_{\alpha,\beta-\frac{1}{2}}}{\Delta y},\ \delta_u\delta_v U^n_{\alpha,\beta} = \delta_u(\delta_v U^n_{\alpha,\beta}),\end{aligned} \tag{26}$$

where u and v can be taken as $x-$ or $y-$directions. For the grid function $U^n_{\alpha,\beta}$, we may omit the subscript if there is no confusion.

Then for grid functions defined on the staggered grid $U := \{U_{i,j}\}$, $V := \{V_{i,j+\frac{1}{2}}\}$, $W := \{W_{i+\frac{1}{2},j}\}$ and $\mathbf{F} := \{(V_{i,j+\frac{1}{2}}, W_{i+\frac{1}{2},j})\}$, the discrete L^2 norms are defined as

$$\begin{aligned}||U||^2_E &= \sum_{j=0}^{J-1}\sum_{i=0}^{I-1} U^2_{i,j}\Delta x\Delta y, \quad ||V||^2_{H_x} = \sum_{j=0}^{J-1}\sum_{i=0}^{I-1} V^2_{i,j+\frac{1}{2}}\Delta x\Delta y,\\ ||W||^2_{H_y} &= \sum_{j=0}^{J-1}\sum_{i=0}^{I-1} W^2_{i+\frac{1}{2},j}\Delta x\Delta y, \quad ||F||^2_H = ||V||^2_{H_x} + ||W||^2_{H_y}.\end{aligned} \tag{27}$$

The equations (17)-(22) can be split into the following forms in each time interval $[t_n, t_{n+1}]$:

$$\left\{\begin{array}{l}\frac{\epsilon_0}{2}\frac{\partial E_z}{\partial t} = -\frac{\partial H_x}{\partial y} - J_z\\ \mu_0\frac{\partial H_x}{\partial t} = -\frac{\partial E_z}{\partial y} - K_x\\ \frac{\partial K_x}{\partial t} + \Gamma_m K_x = \mu_0\omega^2_{pm}H_x\\ \frac{\partial J_z}{\partial t} + \Gamma_e J_z = \epsilon_0\omega^2_{pe}E_z\end{array}\right. \ and\ \left\{\begin{array}{l}\frac{\epsilon_0}{2}\frac{\partial E_z}{\partial t} = \frac{\partial H_y}{\partial x}\\ \mu_0\frac{\partial H_y}{\partial t} = \frac{\partial E_z}{\partial x} - K_y\\ \frac{\partial K_y}{\partial t} + \Gamma_m K_y = \mu_0\omega^2_{pm}H_y\end{array}\right. . \tag{28}$$

Applying the spatial discretization approximation on the staggered grid, we propose the energy-conserved splitting finite-difference time-domain method (EC-S-FDTD) as follows.

Stage 1 : Compute the intermediate variables E^*_z, H^{n+1}_x, K^{n+1}_x and J^{n+1}_z from E^n_z, H^n_x, K^n_x and J^n_z by

$$\epsilon_0\frac{E^*_{z_{i,j}} - E^n_{z_{i,j}}}{\Delta t} = -\frac{1}{2}\delta_y\{H^n_{x_{i,j+\frac{1}{2}}} + H^{n+1}_{x_{i,j+\frac{1}{2}}}\} - \frac{1}{2}(J^n_{z_{i,j}} + J^{n+1}_{z_{i,j}}), \tag{29}$$

$$\mu_0\frac{H^{n+1}_{x_{i,j+\frac{1}{2}}} - H^n_{x_{i,j+\frac{1}{2}}}}{\Delta t} = -\frac{1}{2}\delta_y\{E^n_{z_{i,j+\frac{1}{2}}} + E^*_{z_{i,j+\frac{1}{2}}}\} - \frac{1}{2}(K^{n+1}_{x_{i,j+\frac{1}{2}}} + K^n_{x_{i,j+\frac{1}{2}}}), \tag{30}$$

$$\frac{K^{n+1}_{x_{i,j+\frac{1}{2}}} - K^n_{x_{i,j+\frac{1}{2}}}}{\Delta t} + \frac{\Gamma_m}{2}(K^{n+1}_{x_{i,j+\frac{1}{2}}} + K^n_{x_{i,j+\frac{1}{2}}}) = \frac{\mu_0\omega^2_{pm}}{2}(H^{n+1}_{x_{i,j+\frac{1}{2}}} + H^n_{x_{i,j+\frac{1}{2}}}), \tag{31}$$

$$\frac{J^{n+1}_{z_{i,j}} - J^n_{z_{i,j}}}{\Delta t} + \frac{\Gamma_e}{2}(J^{n+1}_{z_{i,j}} + J^n_{z_{i,j}}) = \frac{\epsilon_0\omega^2_{pe}}{2}(E^n_{z_{i,j}} + E^*_{z_{i,j}}); \tag{32}$$

Stage 2 : Compute the variables E_z^{n+1}, H_y^{n+1} and K_y^{n+1} from E_z^*, H_y^n and K_y^n by

$$\epsilon_0 \frac{E_{z_{i,j}}^{n+1} - E_{z_{i,j}}^*}{\Delta t} = \frac{1}{2}\delta_x\{H_{y_{i,j}}^n + H_{y_{i,j}}^{n+1}\}, \tag{33}$$

$$\mu_0 \frac{H_{y_{i+\frac{1}{2},j}}^{n+1} - H_{y_{i+\frac{1}{2},j}}^n}{\Delta t} = \frac{1}{2}\delta_x\{E_{z_{i+\frac{1}{2},j}}^* + E_{z_{i+\frac{1}{2},j}}^{n+1}\} - \frac{1}{2}(K_{y_{i+\frac{1}{2},j}}^n + K_{y_{i+\frac{1}{2},j}}^{n+1}), \tag{34}$$

$$\frac{K_{y_{i+\frac{1}{2},j}}^{n+1} - K_{y_{i+\frac{1}{2},j}}^n}{\Delta t} + \frac{\Gamma_m}{2}(K_{y_{i+\frac{1}{2},j}}^n + K_{y_{i+\frac{1}{2},j}}^{n+1}) = \frac{\mu_0\omega_{pm}^2}{2}(H_{y_{i+\frac{1}{2},j}}^n + H_{y_{i+\frac{1}{2},j}}^{n+1}). \tag{35}$$

The boundary conditions are

$$\begin{aligned} &E_{z_{0,j}}^* = E_{z_{I,j}}^* = E_{z_{i,0}}^* = E_{z_{i,J}}^* = 0,\\ &E_{z_{0,j}}^{n+1} = E_{z_{I,j}}^{n+1} = E_{z_{i,0}}^{n+1} = E_{z_{i,J}}^{n+1} = 0. \end{aligned} \tag{36}$$

The initial conditions are

$$E_{z_{i,j}}^0 = E_0(x_i, y_j),\ H_{x_{i,j+\frac{1}{2}}}^0 = H_{x0}(x_i, y_{j+\frac{1}{2}}),\ H_{y_{i+\frac{1}{2},j}}^0 = H_{y0}(x_{i+\frac{1}{2}}, y_j). \tag{37}$$

Remark 2: The proposed two-step EC-S-FDTD scheme can be solved conveniently. For Stage 1, The scheme of (29) can be easily to rewrite as a tri-diagonal linear system of E_z^* with the PEC boundary conditions (36) by replacing the relations of (30) (31) and (32) into (29), where the Thomas' algorithm can be used to solve the tri-diagonal linear system, and then from obtained E_z^*, other H_x, J_z, and K_x can be further calculated from (30) (31)(32). Similarly, Stage 2 can be easily solved. The important feature is that the proposed scheme preserves the energy conservation for all time and is unconditionally stable, which we will strictly prove in the next section. The error estimates will also be analyzed in the following sections.

4. The discrete energy conservation

In this section, we will analyze the energy-conserved property of the proposed scheme.

Theorem 2. *(Discrete energy conservation) For the integers $n > 0$, let $\mathbf{H}^n := \{(H_{x_{i,j+\frac{1}{2}}}^n, H_{y_{i+\frac{1}{2},j}}^n)\}$ and $E_z^n := \{E_{z_{i,j}}^n\}$ be the solutions of the scheme (29)-(37). Then it satisfies the energy conservation in the discrete form that for $n \geq 0$*

$$\begin{aligned} &||\epsilon_0^{\frac{1}{2}} E_z^{n+1}||_E^2 + ||\mu_0^{\frac{1}{2}}\mathbf{H}^{n+1}||_H^2 + ||\frac{1}{\epsilon_0{}^{\frac{1}{2}}\omega_{pe}} J_z^{n+1}||_E^2 + ||\frac{1}{\mu_0{}^{\frac{1}{2}}\omega_{pm}}\mathbf{K}^{n+1}||_H^2 \\ &+ \sum_{i=0}^{n-1} 2\Delta t\Gamma_e ||\frac{1}{\epsilon_0{}^{\frac{1}{2}}\omega_{pe}} J_z^{i+\frac{1}{2}}||_E^2 + \sum_{i=0}^{n-1} 2\Delta t\Gamma_m ||\frac{1}{\mu_0{}^{\frac{1}{2}}\omega_{pm}}\mathbf{K}^{i+\frac{1}{2}}||_H^2 \\ &= ||\epsilon_0^{\frac{1}{2}} E_z^0||_E^2 + ||\mu_0^{\frac{1}{2}}\mathbf{H}^0||_H^2 + ||\frac{1}{\epsilon_0{}^{\frac{1}{2}}\omega_{pe}} J_z^0||_E^2 + ||\frac{1}{\epsilon_0{}^{\frac{1}{2}}\omega_{pm}}\mathbf{K}^0||_H^2, \end{aligned} \tag{38}$$

where $f^{i+\frac{1}{2}} = \frac{f^i + f^{i+1}}{2}$.

Proof. Multiplying both sides of (29) with $\Delta t(E_{z_{i,j}}^* + E_{z_{i,j}}^n)$ and multiplying both sides of (30) with $\Delta t(H_{x_{i,j+\frac{1}{2}}}^{n+1} + H_{x_{i,j+\frac{1}{2}}}^n)$, we can get:

$$\begin{aligned} \epsilon_0(E_{z_{i,j}}^{*^2} - E_{z_{i,j}}^{n^2}) &= -\frac{\Delta t}{2}\delta_y\{H_{x_{i,j}}^* + H_{x_{i,j}}^n\}(E_{z_{i,j}}^* + E_{z_{i,j}}^n) \\ &\quad -\frac{\Delta t}{2}(J_{z_{i,j}}^n + J_{z_{i,j}}^{n+1})(E_{z_{i,j}}^* + E_{z_{i,j}}^n), \end{aligned} \tag{39}$$

$$\begin{aligned}\mu_0(H_{x_{i,j+\frac12}}^{n+1^2} - H_{x_{i,j+\frac12}}^{n^2}) &= -\frac{\Delta t}{2}\delta_y\{E^*_{z_{i,j+\frac12}} + E^n_{z_{i,j+\frac12}}\}(H^{n+1}_{x_{i,j+\frac12}} + H^n_{x_{i,j+\frac12}}) \\ &\quad -\frac{\Delta t}{2}(K^{n+1}_{x_{i,j+\frac12}} + K^n_{x_{i,j+\frac12}})(H^{n+1}_{x_{i,j+\frac12}} + H^n_{x_{i,j+\frac12}}). \qquad (40)\end{aligned}$$

From (31) and (32), we have

$$H^{n+1}_{x_{i,j+\frac12}} + H^n_{x_{i,j+\frac12}} = \frac{2}{\Delta t\mu_0\omega_{pm}^2}(K^{n+1}_{x_{i,j+\frac12}} - K^n_{x_{i,j+\frac12}}) + \frac{\Gamma_m}{\mu_0\omega_{pm}^2}(K^{n+1}_{x_{i,j+\frac12}} + K^n_{x_{i,j+\frac12}}),$$

$$E^*_{z_{i,j}} + E^n_{z_{i,j}} = \frac{2}{\Delta t\epsilon_0\omega_{pe}^2}(J^{n+1}_{z_{i,j}} - J^n_{z_{i,j}}) + \frac{\Gamma_e}{\epsilon_0\omega_{pe}^2}(J^{n+1}_{z_{i,j}} + J^n_{z_{i,j}}).$$

Substituting the above relations into (39) and (40), summing over all terms in these two equations and adding them together, we get that

$$\begin{aligned}&(41)\quad \epsilon_0||E^*_z||^2_E - \epsilon_0||E^n_z||^2_E + \mu_0||H^{n+1}_x||^2_{H_x} - \mu_0||H^n_x||^2_{H_x} \\ &= -\sum_{j=0}^{J-1}\sum_{i=0}^{I-1}\Big[\frac{1}{\epsilon_0\omega_{pe}^2}(J^{n+1^2}_{z_{i,j}} - J^{n^2}_{z_{i,j}}) + \frac{\Delta t\Gamma_e}{2\epsilon_0\omega_{pe}^2}(J^n_{z_{i,j}} + J^{n+1}_{z_{i,j}})^2\Big]\Delta x\Delta y \\ &\quad -\sum_{j=0}^{J-1}\sum_{i=0}^{I-1}\Big[\frac{1}{\mu_0\omega_{pm}^2}(K^{n+1^2}_{x_{i,j+\frac12}} - K^{n^2}_{x_{i,j+\frac12}}) + \frac{\Delta t\Gamma_m}{2\mu_0\omega_{pm}^2}(K^n_{x_{i,j+\frac12}} + K^{n+1}_{x_{i,j+\frac12}})^2\Big]\Delta x\Delta y \\ &= -\frac{1}{\epsilon_0\omega_{pe}^2}(||J^{n+1}_z||^2_E - ||J^n_z||^2_E) - \frac{2\Delta t\Gamma_e}{\epsilon_0\omega_{pe}^2}||\frac{J^n_z + J^{n+1}_z}{2}||^2_E \\ &\quad -\frac{1}{\mu_0\omega_{pm}^2}(||K^{n+1}_x||^2_{H_x} - ||K^n_x||^2_{H_x}) - \frac{2\Delta t\Gamma_m}{\mu_0\omega_{pm}^2}||\frac{K^n_x + K^{n+1}_x}{2}||^2_{H_x}.\end{aligned}$$

Similarly treating equations (33)-(37), we obtain that

$$\begin{aligned}&(42)\quad \epsilon_0||E^{n+1}_z||^2_E - \epsilon_0||E^*_z||^2_E + \mu_0||H^{n+1}_y||^2_{H_y} - \mu_0||H^n_y||^2_{H_y} \\ &= -\sum_{j=0}^{J-1}\sum_{i=0}^{I-1}\Big[\frac{1}{\mu_0\omega_{pm}^2}(K^{n+1^2}_{y_{i+\frac12,j}} - K^{n^2}_{y_{i+\frac12,j}}) + \frac{\Delta t\Gamma_m}{2\mu_0\omega_{pm}^2}(K^n_{y_{i+\frac12,j}} + K^{n+1}_{y_{i+\frac12,j}})^2\Big]\Delta x\Delta y \\ &= -\frac{1}{\mu_0\omega_{pm}^2}(||K^{n+1}_y||^2_{H_y} - ||K^n_y||^2_{H_y}) - \frac{2\Delta t\Gamma_m}{\mu_0\omega_{pm}^2}||\frac{K^n_y + K^{n+1}_y}{2}||^2_{H_y}.\end{aligned}$$

Combining equations (41) with (42), we finally have that for any $n \geq 0$

$$\begin{aligned}&\epsilon_0||E^{n+1}_z||^2_E + \mu_0||H^{n+1}_x||^2_{H_x} + \mu_0||H^{n+1}_y||^2_{H_y} + \frac{1}{\mu_0\omega_{pm}^2}||K^{n+1}_x||^2_{H_x} \\ &\quad + \frac{1}{\mu_0\omega_{pm}^2}||K^{n+1}_y||^2_{H_y} + \frac{1}{\epsilon_0\omega_{pe}^2}||J^{n+1}_z||^2_E + \frac{2\Delta t\Gamma_m}{\mu_0\omega_{pm}^2}||\frac{K^n_x + K^{n+1}_x}{2}||^2_{H_x} \\ &\quad + \frac{2\Delta t\Gamma_m}{\mu_0\omega_{pm}^2}||\frac{K^n_y + K^{n+1}_y}{2}||^2_{H_y} + \frac{2\Delta t\Gamma_e}{\epsilon_0\omega_{pe}^2}||\frac{J^n_z + J^{n+1}_z}{2}||^2_E \\ &= \epsilon_0||E^n_z||^2_E + \mu_0||H^n_x||^2_{H_x} + \mu_0||H^n_y||^2_{H_y} + \frac{1}{\mu_0\omega_{pm}^2}||K^n_x||^2_{H_x} \\ &\quad + \frac{1}{\mu_0\omega_{pm}^2}||K^n_y||^2_{H_y} + \frac{1}{\epsilon_0\omega_{pe}^2}||J^n_z||^2_E. \qquad (43)\end{aligned}$$

Summing (43) overall all n from 0 to n leads to (38). This ends the proof. □

From Theorem 2, we can have the following stability result.

Theorem 3. *(Unconditional stability) The proposed scheme (29)-(37) is unconditionally stable.*

5. Convergence analysis

In order to analyze the error estimates of our scheme (29)-(37), we first derive the truncation errors of the scheme by finding an equivalent scheme.

From equations (29) and (33), we get the expression of E_z^*

$$\begin{aligned} E^*_{z_{i,j}} \;=\; & \frac{1}{2}\Big\{(E^n_{z_{i,j}}+E^{n+1}_{z_{i,j}})-\frac{\Delta t}{2\epsilon_0}\delta_y(H^n_{x_{i,j}}+H^{n+1}_{x_{i,j}})-\frac{\Delta t}{2\epsilon_0}\delta_x(H^n_{y_{i,j}}+H^{n+1}_{y_{i,j}}) \\ & -\frac{\Delta t}{2\epsilon_0}(J^n_{z_{i,j}}+J^{n+1}_{z_{i,j}})\Big\}. \end{aligned} \tag{44}$$

Combining (29)-(37) with (44), we derive the following equivalent forms of the EC-S-FDTD scheme

$$\epsilon_0\frac{E^{n+1}_{z_{i,j}}-E^n_{z_{i,j}}}{\Delta t}=-\frac{1}{2}\delta_y(H^n_{x_{i,j}}+H^{n+1}_{x_{i,j}})+\frac{1}{2}\delta_x(H^n_{y_{i,j}}+H^{n+1}_{y_{i,j}})-\frac{1}{2}(J^n_{z_{i,j}}+J^{n+1}_{z_{i,j}}), \tag{45}$$

$$\begin{aligned} \mu_0\frac{H^{n+1}_{x_{i,j+\frac12}}-H^n_{x_{i,j+\frac12}}}{\Delta t} =& -\frac{1}{4}\delta_y(3E^n_{z_{i,j+\frac12}}+E^{n+1}_{z_{i,j+\frac12}})+\frac{\Delta t}{8\epsilon_0}\delta_y\delta_y(H^n_{x_{i,j+\frac12}}+H^{n+1}_{x_{i,j+\frac12}}) \\ & +\frac{\Delta t}{8\epsilon_0}\delta_y\delta_x(H^n_{y_{i,j+\frac12}}+H^{n+1}_{y_{i,j+\frac12}})+\frac{\Delta t}{8\epsilon_0}\delta_y(J^n_{z_{i,j+\frac12}}+J^{n+1}_{z_{i,j+\frac12}}) \\ & -\frac{1}{2}(K^n_{x_{i,j+\frac12}}+K^{n+1}_{x_{i,j+\frac12}}), \end{aligned} \tag{46}$$

$$\begin{aligned} \mu_0\frac{H^{n+1}_{y_{i+\frac12,j}}-H^n_{y_{i+\frac12,j}}}{\Delta t} =& \frac{1}{4}\delta_x(E^n_{z_{i+\frac12,j}}+3E^{n+1}_{z_{i+\frac12,j}})-\frac{\Delta t}{8\epsilon_0}\delta_x\delta_y(H^n_{x_{i+\frac12,j}}+H^{n+1}_{x_{i+\frac12,j}}) \\ & -\frac{\Delta t}{8\epsilon_0}\delta_x\delta_x(H^n_{y_{i+\frac12,j}}+H^{n+1}_{y_{i+\frac12,j}})-\frac{\Delta t}{8\epsilon_0}\delta_x(J^n_{z_{i+\frac12,j}}+J^{n+1}_{z_{i+\frac12,j}}) \\ & -\frac{1}{2}(K^n_{y_{i+\frac12,j}}+K^{n+1}_{y_{i+\frac12,j}}), \end{aligned} \tag{47}$$

$$\frac{K^{n+1}_{x_{i,j+\frac12}}-K^n_{x_{i,j+\frac12}}}{\Delta t}+\frac{\Gamma_m}{2}(K^{n+1}_{x_{i,j+\frac12}}+K^n_{x_{i,j+\frac12}})=\frac{\mu_0\omega^2_{pm}}{2}(H^{n+1}_{x_{i,j+\frac12}}+H^n_{x_{i,j+\frac12}}), \tag{48}$$

$$\frac{K^{n+1}_{y_{i+\frac12,j}}-K^n_{y_{i+\frac12,j}}}{\Delta t}+\frac{\Gamma_m}{2}(K^n_{y_{i+\frac12,j}}+K^{n+1}_{y_{i+\frac12,j}})=\frac{\mu_0\omega^2_{pm}}{2}(H^n_{y_{i+\frac12,j}}+H^{n+1}_{y_{i+\frac12,j}}), \tag{49}$$

$$\begin{aligned} \frac{J^{n+1}_{z_{i,j}}-J^n_{z_{i,j}}}{\Delta t}+\frac{\Gamma_e}{2}(J^{n+1}_{z_{i,j}}+J^n_{z_{i,j}})=&\frac{\epsilon_0\omega^2_{pe}}{4}\Big[3E^n_{z_{i,j}}+E^{n+1}_{z_{i,j}}-\frac{\Delta t}{2\epsilon_0}\delta_y(H^n_{x_{i,j}}+H^{n+1}_{x_{i,j}}) \\ & -\frac{\Delta t}{2\epsilon_0}\delta_x(H^n_{y_{i,j}}+H^{n+1}_{y_{i,j}})-\frac{\Delta t}{2\epsilon_0}(J^n_{z_{i,j}}+J^{n+1}_{z_{i,j}})\Big]. \end{aligned} \tag{50}$$

Let $\eta_{1_{i,j}}^{n+\frac12}$, $\eta_{2_{i,j+\frac12}}^{n+\frac12}$, $\eta_{3_{i+\frac12,j}}^{n+\frac12}$, $\eta_{4_{i,j+\frac12}}^{n+\frac12}$, $\eta_{5_{i+\frac12,j}}^{n+\frac12}$ and $\eta_{6_{i,j}}^{n+\frac12}$ be the truncation errors of the equivalent scheme (45)-(50). Fo obtaining the estimatees of η_1 - η_6, we consider the following auxiliary scheme without right-sided modified terms, i.e.,

$$\epsilon_0\frac{E^{n+1}_{z_{i,j}}-E^n_{z_{i,j}}}{\Delta t}=-\frac{1}{2}\delta_y(H^n_{x_{i,j}}+H^{n+1}_{x_{i,j}})+\frac{1}{2}\delta_x(H^n_{y_{i,j}}+H^{n+1}_{y_{i,j}})-\frac{1}{2}(J^n_{z_{i,j}}+J^{n+1}_{z_{i,j}}), \tag{51}$$

$$\mu_0 \frac{H^{n+1}_{x_{i,j+\frac{1}{2}}} - H^n_{x_{i,j+\frac{1}{2}}}}{\Delta t} = -\frac{1}{4}\delta_y(3E^n_{z_{i,j+\frac{1}{2}}} + E^{n+1}_{z_{i,j+\frac{1}{2}}}) - \frac{1}{2}(K^n_{x_{i,j+\frac{1}{2}}} + K^{n+1}_{x_{i,j+\frac{1}{2}}}), \tag{52}$$

$$\mu_0 \frac{H^{n+1}_{y_{i+\frac{1}{2},j}} - H^n_{y_{i+\frac{1}{2},j}}}{\Delta t} = \frac{1}{4}\delta_x(E^n_{z_{i+\frac{1}{2},j}} + 3E^{n+1}_{z_{i+\frac{1}{2},j}}) - \frac{1}{2}(K^n_{y_{i+\frac{1}{2},j}} + K^{n+1}_{y_{i+\frac{1}{2},j}}), \tag{53}$$

$$\frac{K^{n+1}_{x_{i,j+\frac{1}{2}}} - K^n_{x_{i,j+\frac{1}{2}}}}{\Delta t} + \frac{\Gamma_m}{2}(K^{n+1}_{x_{i,j+\frac{1}{2}}} + K^n_{x_{i,j+\frac{1}{2}}}) = \frac{\mu_0\omega^2_{pm}}{2}(H^{n+1}_{x_{i,j+\frac{1}{2}}} + H^n_{x_{i,j+\frac{1}{2}}}), \tag{54}$$

$$\frac{K^{n+1}_{y_{i+\frac{1}{2},j}} - K^n_{y_{i+\frac{1}{2},j}}}{\Delta t} + \frac{\Gamma_m}{2}(K^n_{y_{i+\frac{1}{2},j}} + K^{n+1}_{y_{i+\frac{1}{2},j}}) = \frac{\mu_0\omega^2_{pm}}{2}(H^n_{y_{i+\frac{1}{2},j}} + H^{n+1}_{y_{i+\frac{1}{2},j}}), \tag{55}$$

$$\frac{J^{n+1}_{z_{i,j}} - J^n_{z_{i,j}}}{\Delta t} + \frac{\Gamma_e}{2}(J^{n+1}_{z_{i,j}} + J^n_{z_{i,j}}) = \frac{\epsilon_0\omega^2_{pe}}{4}\big[3E^n_{z_{i,j}} + E^{n+1}_{z_{i,j}}. \tag{56}$$

Let $\xi^{n+\frac{1}{2}}_{1_{i,j}}$, $\xi^{n+\frac{1}{2}}_{2_{i,j+\frac{1}{2}}}$, $\xi^{n+\frac{1}{2}}_{3_{i+\frac{1}{2},j}}$, $\xi^{n+\frac{1}{2}}_{4_{i,j+\frac{1}{2}}}$, $\xi^{n+\frac{1}{2}}_{5_{i+\frac{1}{2},j}}$ and $\xi^{n+\frac{1}{2}}_{6_{i,j}}$ be the truncation errors of the auxiliary scheme (51)-(56). By using Taylor's expansions, we can obtain that

$$|\xi^{n+\frac{1}{2}}_1|, |\xi^{n+\frac{1}{2}}_2|, \ldots, |\xi^{n+\frac{1}{2}}_6| = O(\Delta t + \Delta x^2 + \Delta y^2). \tag{57}$$

Then for the equivalent scheme (45)-(50), the corresponding truncation errors can be represented and estimated conveniently. In detail, we have that

$$\eta^{n+\frac{1}{2}}_{1_{i,j}} = \xi^{n+\frac{1}{2}}_{1_{i,j}}, \quad \eta^{n+\frac{1}{2}}_{4_{i,j+\frac{1}{2}}} = \xi^{n+\frac{1}{2}}_{4_{i,j+\frac{1}{2}}}, \quad \eta^{n+\frac{1}{2}}_{5_{i+\frac{1}{2},j}} = \xi^{n+\frac{1}{2}}_{5_{i+\frac{1}{2},j}}, \tag{58}$$

$$\begin{aligned} \eta^{n+\frac{1}{2}}_{2_{i,j+\frac{1}{2}}} &= \xi^{n+\frac{1}{2}}_{2_{i,j+\frac{1}{2}}} - \frac{\Delta t}{8\epsilon_0}\delta_y\delta_y\big(H_x(x_i, y_{j+\frac{1}{2}}, t^n) + H_x(x_i, y_{j+\frac{1}{2}}, t^{n+1})\big) \\ &\quad -\frac{\Delta t}{8\epsilon_0}\delta_y\delta_x\big(H_y(x_i, y_{j+\frac{1}{2}}, t^n) + H_y(x_i, y_{j+\frac{1}{2}}, t^{n+1})\big) \\ &\quad -\frac{\Delta t}{8\epsilon_0}\delta_y\big(J_z(x_i, y_{j+\frac{1}{2}}, t^n) + J_z(x_i, y_{j+\frac{1}{2}}, t^{n+1})\big) \end{aligned} \tag{59}$$

$$\begin{aligned} \eta^{n+\frac{1}{2}}_{3_{i+\frac{1}{2},j}} &= \xi^{n+\frac{1}{2}}_{3_{i+\frac{1}{2},j}} + \frac{\Delta t}{8\epsilon_0}\delta_x\delta_y(H^n_{x_{i+\frac{1}{2},j}} + H^{n+1}_{x_{i+\frac{1}{2},j}}) \\ &\quad +\frac{\Delta t}{8\epsilon_0}\delta_x\delta_x(H^n_{y_{i+\frac{1}{2},j}} + H^{n+1}_{y_{i+\frac{1}{2},j}}) + \frac{\Delta t}{8\epsilon_0}\delta_x(J^n_{z_{i+\frac{1}{2},j}} + J^{n+1}_{z_{i+\frac{1}{2},j}}) \end{aligned} \tag{60}$$

$$\begin{aligned} \eta^{n+\frac{1}{2}}_{6_{i,j}} &= \eta^{n+\frac{1}{2}}_{6_{i,j}} + \frac{\epsilon_0\omega^2_{pe}}{4}\big[\frac{\Delta t}{2\epsilon_0}\delta_y(H^n_{x_{i,j}} + H^{n+1}_{x_{i,j}}) + \frac{\Delta t}{2\epsilon_0}\delta_x(H^n_{y_{i,j}} + H^{n+1}_{y_{i,j}}) \\ &\quad +\frac{\Delta t}{2\epsilon_0}(J^n_{z_{i,j}} + J^{n+1}_{z_{i,j}})\big] \end{aligned} \tag{61}$$

From the above estimations (58)-(61), we have the following theorem.

Theorem 4. *(Truncation errors) Assume that the solutions are smooth enough, such that* $E_z \in C^3([0,T]; C^3(\overline{\Omega}))$, $\mathbf{H} \in C^3([0,T]; C^4(\overline{\Omega}))$, $J_z \in C^2([0,T]; C^2(\overline{\Omega}))$, $\mathbf{K} \in C([0,T]; C(\overline{\Omega}))$. *Then the truncation errors of the scheme (29)-(37) are first order in time and second order in space, i.e.,*

(62)

$$\max_{0\le n\le N-1}\big\{|\eta^{n+\frac{1}{2}}_1|, |\eta^{n+\frac{1}{2}}_2|, |\eta^{n+\frac{1}{2}}_3|, |\eta^{n+\frac{1}{2}}_4|, |\eta^{n+\frac{1}{2}}_5|, |\eta^{n+\frac{1}{2}}_6|\big\} \le M\big\{\Delta t + \Delta x^2 + \Delta y^2\big\},$$

where M is independent of steps Δx, Δy and Δt.

In order to get the system of the error equations, we define the intermediate variable $E_z^*(x,y)$ from the exact solution variables.

(63)

$$E_z^*(x,y) = \frac{1}{2}\big\{(E_z(x,y,t^n) + E_z(x,y,t^{n+1})) - \frac{\Delta t}{2\epsilon_0}\delta_y(H_x(x,y,t^n) + H_x(x,y,t^{n+1})) - \frac{\Delta t}{2\epsilon_0}\delta_x(H_y(x,y,t^n) + H_y(x,y,t^{n+1})) - \frac{\Delta t}{2\epsilon_0}(J_z(x,y,t^n) + J_z(x,y,t^{n+1}))\big\}.$$

In addition, we denote the errors as follows

$$\begin{aligned}
&\mathcal{H}^n_{x_{i,j+\frac12}} = H_x(x_i, y_{j+\frac12}, t^n) - H^n_{x_{i,j+\frac12}}, \quad \mathcal{H}^n_{y_{i+\frac12,j}} = H_y(x_{i+\frac12}, y_j, t^n) - H^n_{y_{i+\frac12,j}},\\
&\mathcal{E}^n_{z_{i,j}} = E_z(x_i, y_j, t^n) - E^n_{z_{i,j}}, \quad \mathcal{K}^n_{x_{i,j+\frac12}} = K_x(x_i, y_{j+\frac12}, t^n) - K^n_{x_{i,j+\frac12}},\\
&\mathcal{K}^n_{y_{i+\frac12,j}} = K_y(x_{i+\frac12}, y_j, t^n) - K^n_{y_{i+\frac12,j}}, \quad \mathcal{J}^n_{z_{i,j}} = J_z(x_i, y_j, t^n) - J^n_{z_{i,j}},\\
&\mathcal{E}^*_{z_{i,j}} = E^*_z(x_i, y_j) - E^*_{z_{i,j}}.
\end{aligned}$$

By the definition of the intermediate variables $E^*_{z_{i,j}}$ in (44), and $E_z^*(x,y,t)$ in (63), we can derive the system of the error equations of the EC-S-FDTD scheme as follows.

Stage 1:

$$\epsilon_0\frac{\mathcal{E}^*_{z_{i,j}} - \mathcal{E}^n_{z_{i,j}}}{\Delta t} = -\frac{1}{2}\delta_y\{\mathcal{H}^n_{x_{i,j+\frac12}} + \mathcal{H}^{n+1}_{x_{i,j+\frac12}}\} - \frac{1}{2}(\mathcal{J}^n_{z_{i,j}} + \mathcal{J}^{n+1}_{z_{i,j}}) + e^{n+\frac12}_{1_{i,j}}, \tag{64}$$

(65)

$$\mu_0\frac{\mathcal{H}^{n+1}_{x_{i,j+\frac12}} - \mathcal{H}^n_{x_{i,j+\frac12}}}{\Delta t} = -\frac{1}{2}\delta_y\{\mathcal{E}^n_{z_{i,j+\frac12}} + \mathcal{E}^*_{z_{i,j+\frac12}}\} - \frac{1}{2}(\mathcal{K}^{n+1}_{x_{i,j+\frac12}} + \mathcal{K}^n_{x_{i,j+\frac12}}) + e^{n+\frac12}_{2_{i,j+\frac12}},$$

(66)

$$\frac{\mathcal{K}^{n+1}_{x_{i,j+\frac12}} - \mathcal{K}^n_{x_{i,j+\frac12}}}{\Delta t} + \frac{\Gamma_m}{2}(\mathcal{K}^{n+1}_{x_{i,j+\frac12}} + \mathcal{K}^n_{x_{i,j+\frac12}}) = \frac{\mu_0\omega^2_{pm}}{2}(\mathcal{H}^{n+1}_{x_{i,j+\frac12}} + \mathcal{H}^n_{x_{i,j+\frac12}}) + e^{n+\frac12}_{3_{i,j+\frac12}},$$

$$\frac{\mathcal{J}^{n+1}_{z_{i,j}} - \mathcal{J}^n_{z_{i,j}}}{\Delta t} + \frac{\Gamma_e}{2}(\mathcal{J}^{n+1}_{z_{i,j}} + \mathcal{J}^n_{z_{i,j}}) = \frac{\epsilon_0\omega^2_{pe}}{2}(\mathcal{E}^n_{z_{i,j}} + \mathcal{E}^*_{z_{i,j}}) + e^{n+\frac12}_{4_{i,j}}, \tag{67}$$

and the boundary conditions

$$\mathcal{E}^*_{z_{0,j}} = \mathcal{E}^*_{z_{I,j}} = \mathcal{E}^*_{z_{i,0}} = \mathcal{E}^*_{z_{i,J}} = 0; \tag{68}$$

Stage 2:

$$\epsilon_0\frac{\mathcal{E}^{n+1}_{z_{i,j}} - \mathcal{E}^*_{z_{i,j}}}{\Delta t} = \frac{1}{2}\delta_x\{\mathcal{H}^*_{y_{i,j}} + \mathcal{H}^{n+1}_{y_{i,j}}\} + e^{n++\frac12}_{5_{i,j}}, \tag{69}$$

(70)

$$\mu_0\frac{\mathcal{H}^{n+1}_{y_{i+\frac12,j}} - \mathcal{H}^*_{y_{i+\frac12,j}}}{\Delta t} = \frac{1}{2}\delta_x\{\mathcal{E}^*_{z_{i+\frac12,j}} + \mathcal{E}^{n+1}_{z_{i+\frac12,j}}\} - \frac{1}{2}(\mathcal{K}^n_{y_{i+\frac12,j}} + \mathcal{K}^{n+1}_{y_{i+\frac12,j}}) + e^{n+\frac12}_{6_{i+\frac12,j}},$$

(71)

$$\frac{\mathcal{K}^{n+1}_{y_{i+\frac12,j}} - \mathcal{K}^n_{y_{i+\frac12,j}}}{\Delta t} + \frac{\Gamma_m}{2}(\mathcal{K}^n_{y_{i+\frac12,j}} + \mathcal{K}^{n+1}_{y_{i+\frac12,j}}) = \frac{\mu_0\omega^2_{pm}}{2}(\mathcal{H}^n_{y_{i+\frac12,j}} + \mathcal{H}^{n+1}_{y_{i+\frac12,j}}) + e^{n+\frac12}_{7_{i+\frac12,j}},$$

and the boundary conditions

$$\mathcal{E}^{n+1}_{z_{0,j}} = \mathcal{E}^{n+1}_{z_{I,j}} = \mathcal{E}^{n+1}_{z_{i,0}} = \mathcal{E}^{n+1}_{z_{i,J}} = 0. \tag{72}$$

Where

$$
\begin{aligned}
&e_{1_{i,j}}^{n+\frac{1}{2}} = \frac{1}{2}\eta_{1_{i,j}}^{n+\frac{1}{2}}, \quad e_{2_{i,j+\frac{1}{2}}}^{n+\frac{1}{2}} = \eta_{2_{i,j+\frac{1}{2}}}^{n+\frac{1}{2}}, \quad e_{3_{i,j+\frac{1}{2}}}^{n+\frac{1}{2}} = \eta_{3_{i,j+\frac{1}{2}}}^{n+\frac{1}{2}}, \quad e_{4_{i,j}}^{n+\frac{1}{2}} = \eta_{4_{i,j}}^{n+\frac{1}{2}},\\
&e_{5_{i,j}}^{n+\frac{1}{2}} = \frac{1}{2}\eta_{1_{i,j}}^{n+\frac{1}{2}}, \quad e_{6_{i+\frac{1}{2},j}}^{n+\frac{1}{2}} = \eta_{5_{i+\frac{1}{2},j}}^{n+\frac{1}{2}}, \quad e_{7_{i+\frac{1}{2},j}}^{n+\frac{1}{2}} = \eta_{6_{i+\frac{1}{2},j}}^{n+\frac{1}{2}}.
\end{aligned} \tag{73}
$$

Theorem 5. *(Convergence) Suppose that the exact solution components of equations (17)-(25), E_z, H_x, H_y, J_z, K_x and K_y, are smooth enough such that $E_z \in C^3([0,T];C^3(\overline{\Omega}))$, $\mathbf{H}\in C^3([0,T];C^4(\overline{\Omega}))$, $J_z\in C^2([0,T];C^2(\overline{\Omega}))$, $\mathbf{K}\in C([0,T];C(\overline{\Omega}))$. For $n\geq 0$, let E_z^n, H_x^n, H_y^n, J_z^n, K_x^n and K_y^n be the solutions of the scheme (29)-(37). Then there exists a positive constant M independent of Δx, Δy and Δt such that*

$$
\begin{aligned}
&\epsilon_0||\mathcal{E}_z^{n+1}||_E^2 + \mu_0||\mathcal{H}^{n+1}||_H^2 + \frac{1}{\mu_0\omega_{pm}^2}||\mathcal{K}^{n+1}||_H^2 + \frac{1}{\epsilon_0\omega_{pe}^2}||\mathcal{J}_z^{n+1}||_E^2\\
&\quad\leq M\big(\epsilon_0||\mathcal{E}_z^0||_E^2 + \mu_0||\mathcal{H}^0||_H^2 + \frac{1}{\mu_0\omega_{pm}^2}||\mathcal{K}^0||_H^2 + \frac{1}{\epsilon_0\omega_{pe}^2}||\mathcal{J}_z^0||_E^2\big)\\
&\qquad + M\big(\Delta t + \Delta x^2 + \Delta y^2\big)^2.
\end{aligned} \tag{74}
$$

Proof. Multiplying both sides of (64) with $\Delta t(\mathcal{E}_{z_{i,j}}^* + \mathcal{E}_{z_{i,j}}^n)$, multiplying both sides of (65) with $\Delta t(\mathcal{H}_{x_{i,j+\frac{1}{2}}}^{n+1} + \mathcal{H}_{x_{i,j+\frac{1}{2}}}^n)$ and then summing them, we can obtain

$$
\begin{aligned}
&\epsilon_0(\mathcal{E}_{z_{i,j}}^{*^2} - \mathcal{E}_{z_{i,j}}^{n^2}) + \mu_0(\mathcal{H}_{x_{i,j+\frac{1}{2}}}^{n+1^2} + \mathcal{H}_{x_{i,j+\frac{1}{2}}}^{n^2}) = -\frac{\Delta t}{2}\delta_y\big\{\mathcal{H}_{x_{i,j+\frac{1}{2}}}^n + \mathcal{H}_{x_{i,j+\frac{1}{2}}}^{n+1}\big\}(\mathcal{E}_{z_{i,j}}^* + \mathcal{E}_{z_{i,j}}^n)\\
&\quad - \frac{\Delta t}{2}(\mathcal{J}_{z_{i,j}}^n + \mathcal{J}_{z_{i,j}}^{n+1})(\mathcal{E}_{z_{i,j}}^* + \mathcal{E}_{z_{i,j}}^n) - \frac{\Delta t}{2}\delta_y\big\{\mathcal{E}_{z_{i,j+\frac{1}{2}}}^n + \mathcal{E}_{z_{i,j+\frac{1}{2}}}^*\big\}(\mathcal{H}_{x_{i,j+\frac{1}{2}}}^{n+1} + \mathcal{H}_{x_{i,j+\frac{1}{2}}}^n)\\
&\quad - \frac{\Delta t}{2}(\mathcal{K}_{x_{i,j+\frac{1}{2}}}^{n+1} + \mathcal{K}_{x_{i,j+\frac{1}{2}}}^n)(\mathcal{H}_{x_{i,j+\frac{1}{2}}}^{n+1} + \mathcal{H}_{x_{i,j+\frac{1}{2}}}^n)\\
&\quad + e_{1_{i,j}}^{n+\frac{1}{2}}(\mathcal{E}_{z_{i,j}}^* + \mathcal{E}_{z_{i,j}}^n)\Delta t + e_{2_{i,j+\frac{1}{2}}}^{n+\frac{1}{2}}(\mathcal{H}_{x_{i,j+\frac{1}{2}}}^{n+1} + \mathcal{H}_{x_{i,j+\frac{1}{2}}}^n)\Delta t.
\end{aligned} \tag{75}
$$

Then multiplying both sides of (67) with $\frac{\Delta t}{\epsilon_0\omega_{pe}^2}(J_{z_{i,j}}^n + J_{z_{i,j}}^{n+1})$ and multiplying both sides of (66) with $\frac{\Delta t}{\mu_0\omega_{pm}^2}(K_{x_{i,j}}^n + K_{x_{i,j}}^{n+1})$, we have that

$$
\frac{J_{z_{i,j}}^{n+1^2} - J_{z_{i,j}}^{n^2}}{\epsilon_0\omega_{pe}^2} + \frac{\Delta t\Gamma_e}{2\epsilon_0\omega_{pe}^2}(J_{z_{i,j}}^n + J_{z_{i,j}}^{n+1})^2 = \frac{\Delta t}{2}(J_{z_{i,j}}^n + J_{z_{i,j}}^{n+1}) + \frac{\Delta t e_{4_{i,j}}^{n+\frac{1}{2}}}{\epsilon_0\omega_{pe}^2}(J_{z_{i,j}}^n + J_{z_{i,j}}^{n+1}), \tag{76}
$$

and

$$
\begin{aligned}
\frac{K_{x_{i,j+\frac{1}{2}}}^{n+1^2} - K_{x_{i,j+\frac{1}{2}}}^{n^2}}{\mu_0\omega_{pm}^2} &+ \frac{\Delta t\Gamma_m}{2\mu_0\omega_{pm}^2}(K_{x_{i,j+\frac{1}{2}}}^n + K_{x_{i,j+\frac{1}{2}}}^{n+1})^2 = \frac{\Delta t}{2}(K_{x_{i,j+\frac{1}{2}}}^n + K_{x_{i,j+\frac{1}{2}}}^{n+1})\\
&+ \frac{\Delta t e_{3_{i,j+\frac{1}{2}}}^{n+\frac{1}{2}}}{\mu_0\omega_{pm}^2}(K_{x_{i,j+\frac{1}{2}}}^n + K_{x_{i,j+\frac{1}{2}}}^{n+1}).
\end{aligned} \tag{77}
$$

Combining (75) with (76) and (77), summing the resulted equation with respect to the argument subscript i and j, and using the boundary conditions (68) and

(72), we obtain that

(78)
$$
\begin{aligned}
&\epsilon_0(||\mathcal{E}_z^*||_E^2-||\mathcal{E}_z^n||_E^2)+\mu_0(||\mathcal{H}_x^{n+1}||_{H_x}^2-||\mathcal{H}_x^n||_{H_x}^2)+\frac{1}{\epsilon_0\omega_{pe}^2}(||\mathcal{J}_z^{n+1}||_E^2-||\mathcal{J}_z^n||_E^2)\\
&+\frac{1}{\mu_0\omega_{pm}^2}(||\mathcal{K}_x^{n+1}||_{H_x}^2-||\mathcal{K}_x^n||_{H_x}^2)+\frac{\Delta t\Gamma_e}{2\epsilon_0\omega_{pe}^2}||\mathcal{J}_z^{n+1}+\mathcal{J}_z^n||_E^2+\frac{\Delta t\Gamma_m}{2\mu_0\omega_{pm}^2}||\mathcal{K}_x^{n+1}+\mathcal{K}_x^n||_{H_x}^2\\
&=\frac{\Delta t}{\epsilon_0\omega_{pe}^2}\sum_{j=0}^{J-1}\sum_{i=0}^{I-1}e_{4_{i,j}}^{n+\frac12}(\mathcal{J}_{z_{i,j}}^{n+1}+\mathcal{J}_{z_{i,j}}^n)+\frac{\Delta t}{\mu_0\omega_{pm}^2}\sum_{j=0}^{J-1}\sum_{i=0}^{I-1}e_{3_{i,j+\frac12}}^{n+\frac12}(\mathcal{K}_{x_{i,j+\frac12}}^{n+1}+\mathcal{K}_{x_{i,j+\frac12}}^n)\\
&\quad+\Delta t\sum_{j=0}^{J-1}\sum_{i=0}^{I-1}e_{1_{i,j}}^{n+\frac12}(\mathcal{E}_{z_{i,j}}^*+\mathcal{E}_{z_{i,j}}^n)+\Delta t\sum_{j=0}^{J-1}\sum_{i=0}^{I-1}e_{2_{i,j+\frac12}}^{n+\frac12}(\mathcal{H}_{x_{i,j+\frac12}}^{n+1}+\mathcal{H}_{x_{i,j+\frac12}}^n).
\end{aligned}
$$

By the Cauchy-inequality, it holds that

$$
\begin{aligned}
&e_{4_{i,j}}^{n+\frac12}(\mathcal{J}_{z_{i,j}}^{n+1}+\mathcal{J}_{z_{i,j}}^n)\le\frac{\Gamma_e}{2}(\mathcal{J}_{z_{i,j}}^{n+1}+\mathcal{J}_{z_{i,j}}^n)^2+\frac{1}{2\Gamma_e}e_{4_{i,j}}^{n+\frac12\,2},\\
&e_{3_{i,j+\frac12}}^{n+\frac12}(\mathcal{K}_{x_{i,j+\frac12}}^{n+1}+\mathcal{K}_{x_{i,j+\frac12}}^n)\le\frac{\Gamma_m}{2}(\mathcal{K}_{x_{i,j+\frac12}}^{n+1}+\mathcal{K}_{x_{i,j+\frac12}}^n)^2+\frac{1}{2\Gamma_m}e_{3_{i,j+\frac12}}^{n+\frac12\,2}.
\end{aligned}
\tag{79}
$$

With the above two relations in (79), we can eliminate the two terms containing Δt on the left side of the equation (78), and get that

(80)
$$
\begin{aligned}
&\epsilon_0(||\mathcal{E}_z^*||_E^2-||\mathcal{E}_z^n||_E^2)+\mu_0(||\mathcal{H}_x^{n+1}||_{H_x}^2-||\mathcal{H}_x^n||_{H_x}^2)+\frac{1}{\epsilon_0\omega_{pe}^2}(||\mathcal{J}_z^{n+1}||_E^2-||\mathcal{J}_z^n||_E^2)\\
&\qquad+\frac{1}{\mu_0\omega_{pm}^2}(||\mathcal{K}_x^{n+1}||_{H_x}^2-||\mathcal{K}_x^n||_{H_x}^2)\\
&\qquad\le\frac{\Delta t}{2\Gamma_e\epsilon_0\omega_{pe}^2}||e_4^{n+\frac12}||_E^2+\frac{\Delta t}{2\Gamma_m\mu_0\omega_{pm}^2}||e_3^{n+\frac12}||_{H_x}^2+\Delta t\big(\frac{1}{\epsilon_0}||e_1^{n+\frac12}||_E^2+\frac{\epsilon_0}{2}||\mathcal{E}_z^*||_E^2\\
&\qquad+\frac{\epsilon_0}{2}||\mathcal{E}_z^n||_E^2+\frac{1}{\mu_0}||e_2^{n+\frac12}||_{H_x}^2+\frac{\mu_0}{2}||\mathcal{H}_x^n||_{H_x}^2+\frac{\mu_0}{2}||\mathcal{H}_x^{n+1}||_{H_x}^2\big).
\end{aligned}
$$

Thus, we have that

(81)
$$
\begin{aligned}
&(1-\frac{\Delta t}{2})\big[\epsilon_0||\mathcal{E}_z^*||_E^2+\mu_0||\mathcal{H}_x^{n+1}||_{H_x}^2+\frac{1}{\epsilon_0\omega_{pe}^2}||\mathcal{J}_z^{n+1}||_E^2+\frac{1}{\mu_0\omega_{pm}^2}||\mathcal{K}_x^{n+1}||_{H_x}^2\big]\\
&\qquad\le(1+\frac{\Delta t}{2})\Big[\epsilon_0||\mathcal{E}_z^n||_E^2+\mu_0||\mathcal{H}_x^n||_{H_x}^2+\frac{1}{\epsilon_0\omega_{pe}^2}||\mathcal{J}_z^n||_E^2+\frac{1}{\mu_0\omega_{pm}^2}||\mathcal{K}_x^n||_{H_x}^2\Big]\\
&\qquad\quad+\frac{\Delta t}{2\Gamma_e\epsilon_0\omega_{pe}^2}||e_4^{n+\frac12}||_E^2+\frac{\Delta t}{2\Gamma_m\mu_0\omega_{pm}^2}||e_3^{n+\frac12}||_{H_x}^2+\frac{\Delta t}{\epsilon_0}||e_1^{n+\frac12}||_E^2+\frac{\Delta t}{\mu_0}||e_2^{n+\frac12}||_{H_x}^2\\
&\qquad\le(1+\frac{\Delta t}{2})\Big[\epsilon_0||\mathcal{E}_z^n||_E^2+\mu_0||\mathcal{H}_x^n||_{H_x}^2+\frac{1}{\epsilon_0\omega_{pe}^2}||\mathcal{J}_z^n||_E^2+\frac{1}{\mu_0\omega_{pm}^2}||\mathcal{K}_x^n||_{H_x}^2\Big]\\
&\qquad\quad+O\big(\Delta t(\Delta t+\Delta x^2+\Delta y^2)^2\big).
\end{aligned}
$$

Similarly, from Stage 2 (69)-(72), we can get that

$$
\begin{aligned}
&(1-\frac{\Delta t}{2})\Big[\epsilon_0||\mathcal{E}_z^{n+1}||_E^2+\mu_0||\mathcal{H}_y^{n+1}||_{H_y}^2+\frac{1}{\mu_0\omega_{pm}^2}||\mathcal{K}_y^{n+1}||_{H_y}^2\Big]\\
&\le(1+\frac{\Delta t}{2})\Big[\epsilon_0||\mathcal{E}_z^{*}||_E^2+\mu_0||\mathcal{H}_y^{n}||_{H_y}^2+\frac{1}{\mu_0\omega_{pm}^2}||\mathcal{K}_y^{n}||_{H_y}^2\Big]\\
&\quad+\frac{\Delta t}{2\Gamma_m\mu_0\omega_{pm}^2}||e_7^{n+\frac12}||_{H_y}^2+\frac{\Delta t}{\epsilon_0}||e_5^{n+\frac12}||_E^2+\frac{\Delta t}{\mu_0}||e_6^{n+\frac12}||_{H_y}^2\\
&\le(1+\frac{\Delta t}{2})\Big[\epsilon_0||\mathcal{E}_z^{*}||_E^2+\mu_0||\mathcal{H}_y^{n}||_{H_y}^2+\frac{1}{\mu_0\omega_{pm}^2}||\mathcal{K}_y^{n}||_{H_y}^2\Big]\\
&\quad+O\big(\Delta t(\Delta t+\Delta x^2+\Delta y^2)^2\big).
\end{aligned}
\tag{82}
$$

Dividing both sides of (81) with $(1-\frac{\Delta t}{2})$ and dividing both sides of (82) with $(1+\frac{\Delta t}{2})$, summing these two inequalities leads to that that

(83)

$$
\begin{aligned}
&\mu_0||\mathcal{H}_x^{n+1}||_{H_x}^2+\frac{1}{\epsilon_0\omega_{pe}^2}||\mathcal{J}_z^{n+1}||_E^2+\frac{1}{\mu_0\omega_{pm}^2}||\mathcal{K}_x^{n+1}||_{H_x}^2+(\frac{1-\frac{\Delta t}{2}}{1+\frac{\Delta t}{2}})\Big[\epsilon_0||\mathcal{E}_z^{n+1}||_E^2\\
&\quad+\mu_0||\mathcal{H}_y^{n+1}||_{H_y}^2+\frac{1}{\mu_0\omega_{pm}^2}||\mathcal{K}_y^{n+1}||_{H_y}^2\Big]\\
&\le\mu_0||\mathcal{H}_y^{n+1}||_{H_y}^2+\frac{1}{\mu_0\omega_{pm}^2}||\mathcal{K}_y^{n}||_{H_y}^2+(\frac{1+\frac{\Delta t}{2}}{1-\frac{\Delta t}{2}})\Big[\epsilon_0||\mathcal{E}_z^{n}||_E^2+\mu_0||\mathcal{H}_x^{n}||_{H_x}^2+\frac{1}{\epsilon_0\omega_{pe}^2}||\mathcal{J}_z^{n}||_E^2\\
&\quad+\frac{1}{\mu_0\omega_{pm}^2}||\mathcal{K}_x^{n}||_{H_x}^2\Big]+O\big(\Delta t(\Delta t+\Delta x^2+\Delta y^2)^2\big).
\end{aligned}
$$

Then, for that $\frac{1-\frac{\Delta t}{2}}{1+\frac{\Delta t}{2}}\ge 1-\Delta t$, we have that

$$
\begin{aligned}
&(1-\Delta t)\Big[\epsilon_0||\mathcal{E}_z^{n+1}||_E^2+\mu_0||\mathcal{H}_x^{n+1}||_{H_x}^2+\mu_0||\mathcal{H}_y^{n+1}||_{H_y}^2+\frac{1}{\epsilon_0\omega_{pe}^2}||\mathcal{J}_z^{n+1}||_E^2\\
&\quad+\frac{1}{\mu_0\omega_{pm}^2}||\mathcal{K}_x^{n+1}||_{H_x}^2+\frac{1}{\mu_0\omega_{pm}^2}||\mathcal{K}_y^{n+1}||_{H_y}^2\Big]\\
&\le(\frac{1+\frac{\Delta t}{2}}{1-\frac{\Delta t}{2}})\Big[\epsilon_0||\mathcal{E}_z^{n}||_E^2+\mu_0||\mathcal{H}_x^{n}||_{H_x}^2+\mu_0||\mathcal{H}_y^{n}||_{H_y}^2+\frac{1}{\epsilon_0\omega_{pe}^2}||\mathcal{J}_z^{n}||_E^2\\
&\quad+\frac{1}{\mu_0\omega_{pm}^2}||\mathcal{K}_x^{n}||_{H_x}^2+\frac{1}{\mu_0\omega_{pm}^2}||\mathcal{K}_y^{n}||_{H_y}^2\Big]+O\big(\Delta t(\Delta t+\Delta x^2+\Delta y^2)^2\big).
\end{aligned}
\tag{84}
$$

Noting that for $0\le n\le N=\frac{T}{\Delta t}$,

$$
\begin{aligned}
&\Big[(\frac{1+\frac{\Delta t}{2}}{1-\frac{\Delta t}{2}})\frac{1}{(1-\Delta t)}\Big]^n\le\Big[(\frac{1+\frac{\Delta t}{2}}{1-\frac{\Delta t}{2}})\frac{1}{(1-\Delta t)}\Big]^N\\
&\quad\le\big(1+\frac{\Delta t}{1-\frac{\Delta t}{2}}\big)^{(\frac{1-\frac{\Delta t}{2}}{\Delta t})\frac{T}{(1-\frac{\Delta t}{2})}}\cdot\big(1+\frac{\Delta t}{1-\Delta t}\big)^{(\frac{1-\Delta t}{\Delta t})\frac{T}{(1-\Delta t)}}\le e^{2T},
\end{aligned}
\tag{85}
$$

and repeating (84) from time level n to 0, we finally obtain conclusion (74). This complete the proof. $\square$

6. Numerical Experiments

In this section, we will give numerical experiments to show the performance of our proposed scheme and also compute the propagation feature of electromagnetic waves in metamaterials.

Example 1. In this example, we test the energy conservation of our EC-S-FDTD scheme and its convergence rates. Let $Energy_n$ be the discrete energy of the numerical solution at t^n as

$$\begin{aligned} Energy_n = &||\epsilon_0^{\frac{1}{2}} E_z^n||_E^2 + ||\mu_0^{\frac{1}{2}} \mathbf{H}^n||_H^2 + ||\frac{1}{\epsilon_0{}^{\frac{1}{2}}\omega_{pe}} J_z^n||_E^2 + ||\frac{1}{\mu_0{}^{\frac{1}{2}}\omega_{pm}} \mathbf{K}^n||_H^2 \\ &+ \sum_{i=1}^{n} 2\Delta t \Gamma_e ||\frac{1}{\epsilon_0{}^{\frac{1}{2}}\omega_{pe}} \frac{J_z^{i-1}+J_z^i}{2}||_E^2 + \sum_{i=1}^{n} 2\Delta t \Gamma_m ||\frac{1}{\mu_0{}^{\frac{1}{2}}\omega_{pm}} \frac{\mathbf{K}^{i-1}+\mathbf{K}^i}{2}||_H^2, \end{aligned} \tag{86}$$

and

$$Energy_0 = ||\epsilon_0^{\frac{1}{2}} E_z^0||_E^2 + ||\mu_0^{\frac{1}{2}} \mathbf{H}^0||_H^2 + ||\frac{1}{\epsilon_0^{\frac{1}{2}}\omega_{pe}} J_z^0||_E^2 + ||\frac{1}{\mu_0^{\frac{1}{2}}\omega_{pm}} ||\mathbf{K}^0||_H^2. \tag{87}$$

Then let the absolute and relative errors of energy be

$$Energy\ Error\ I = \max_{1\le n\le N} \big|Energy_n - Energy_0\big|, \tag{88}$$

$$Energy\ Error\ II = \max_{1\le n\le N} \frac{\big|Energy_n - Energy_0\big|}{Energy_0}. \tag{89}$$

Consider a unit square domain $\Omega = [0,1]\times[0,1]$ and a time interval $[0,1]$. The parameters of metamaterials are set as $\epsilon_0 = \mu_0 = 1$, $\omega_{pe} = \omega_{pm} = 1$, and $\Gamma_e = \Gamma_m = 1$. The initial electromganetic fields are given as

$$E_{z0}(x,y) = \sin\pi x \sin\pi y, \quad H_{x0}(x,y) = \pi \sin\pi x \cos\pi y, \tag{90}$$

$$H_{y0}(x,y) = -\pi \cos\pi x \sin\pi y, \quad J_{z0}(x,y) = 0, \tag{91}$$

$$K_{x0}(x,y) = 0, \quad K_{y0}(x,y) = 0, \tag{92}$$

which satisfy the PEC boundary conditions and the divergence-free condition.

Table 1 shows the numerical errors of the discrete energies with different step sizes. We can see clearly that the *Energy Error I* and *Energy Error II* of the EC-S-FDTD scheme both reach the machine precision. The numerical energies of electromagnetic waves of the scheme are conserved in metamaterials, which confirm the theoretical analysis.

TABLE 1. Energy Conservations of the EC-S-FDTD scheme with different step sizes.

Mesh ($I\times J\times N$)	Error I of Energy	Error II of Energy
$8\times8\times8$	1.7764e-15	7.8012e-16
$16\times16\times16$	7.9936e-15	3.5106e-15
$32\times32\times32$	5.7732e-15	2.5354e-15
$64\times64\times64$	1.5099e-14	6.6311e-15

In order to show the convergence rates in time and space of the EC-S-FDTD scheme, we define *Error I* and *Error II* of the numerical solutions as follows:

$$Error\ I = \max_{0\le n\le N} \big(\epsilon_0 ||[E_z(t^n) - E_z^n]||_E^2 + \mu_0 ||[\mathbf{H}(t^n) - \mathbf{H}^n]||_H^2\big)^{\frac{1}{2}}, \tag{93}$$

and

$$Error\ II = \max_{0\leq n\leq N}\Big(\epsilon_0|||[E_z(t^n) - E_z^n]|||_E^2 + \mu_0|||[\mathbf{H}(t^n) - \mathbf{H}^n]|||_H^2 \tag{94}$$
$$+ \frac{1}{\epsilon_0\omega_{pe}^2}|||[J_z(t^n) - J_z^n||_E^2 + \frac{1}{\mu_0\omega_{pm}^2}|||[\mathbf{K}(t^n) - \mathbf{K}^n||_H^2\Big)^{\frac{1}{2}}.$$

The errors and convergence rates of numerical solutions of the EC-S-FDTD scheme are listed in Tables 2 and 3. As the problem has not exact solution, we use the reference solutions to replace the exact solution in computing the errors in (93) and (94). In the tables, the reference solutions of the system (17)-(25) are computed by using fine meshes of $\Delta x = \Delta y = 1/243$ and $\Delta t = 10^{-4}$.

Table 2. Errors and convergence rate in time of the EC-S-FDTD scheme.

Mesh (N)	Error I	Rate	Error II	Rate
20	2.7591e-2		2.8553e-2	
40	1.3694e-2	1.01	1.4165e-2	1.01
80	6.7552e-3	1.02	6.9859e-3	1.02
160	3.2887e-3	1.04	3.4012e-3	1.04

Table 3. Errors and convergence rate in space of the EC-S-FDTD scheme.

Mesh ($I\times J$)	Error I	Rate	Error II	Rate
3×3	1.3325e-1		1.3439e-1	
9×9	1.4972e-2	1.99	1.5101e-2	1.99
27×27	1.6479e-3	2.01	1.6620e-3	2.01
81×81	1.6500e-4	2.09	1.6653e-4	2.09

From Tables 2 and 3, it is clear to see that our EC-S-FDTD scheme is of first order convergence in time and of second order convergence in space, which is consistent with the theoretical analysis.

Example 2. The problem in double-negative media. We consider a planar double-negative medium slab in the center of the domain. Choosing $\omega_{pe} = \omega_{pm} = \sqrt{2}\omega_0$ and $\Gamma_e = \Gamma_m = 0$ in (4) leads to $\epsilon_r = \mu_r = -1$. A slab with thickness $d = 2\lambda_0$ and width $L = 10\lambda_0$ is employed. And the point source is located $d/2 = \lambda_0$ above the slab interface. In simulation, we take the space step sizes $\Delta x = \Delta y = \lambda_0/100$, where the Courant-Friedrich-Levy number is $C_N = 5$, and set 40-cell PML layer to truncate the computational domain. The snapshots of the contour of electric field intensity at the time $t = 400\Delta t$ obtained by our EC-S-FDTD scheme is showed in Figure 1. In the figures, the gray-scale contours represent different values. The darker (lighter) regions correspond to lower (higher) intensity levels. It can be clearly seen from the figure that at the center of the DNG slab the focus phenomenon happens as well as that of outside the slab, about $d/2$ away from the bottom edge of the slab.

We then simulate the propagation of electromagnetic wave through a lossy "unmatched" double-negative slab ($\epsilon_r = \mu_r \approx -3 - 0.002j$). The numerical results are shown in Figure 2. In this case, the Drude model parameters are $\omega_{pe} = \omega_{pm} = 2\omega_0$ and $\Gamma_e = \Gamma_m = 5.3\times 10^{-4}\omega_0$. In computation, the CFL number $C_N = 5$ is employed

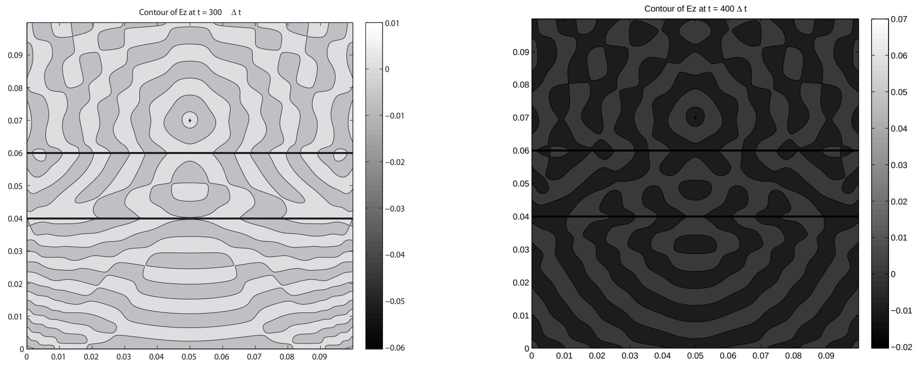

FIGURE 1. Contours of E_z from a point source above a lossless double-negative slab ($\epsilon_r = \mu_r = -1$) with thickness $d = 2\lambda_0$, $\omega_0 = 2\pi f_0$ and $f_0 = 30G$ at $t = 300\Delta t$ (left) and $t = 400\Delta t$ (right).

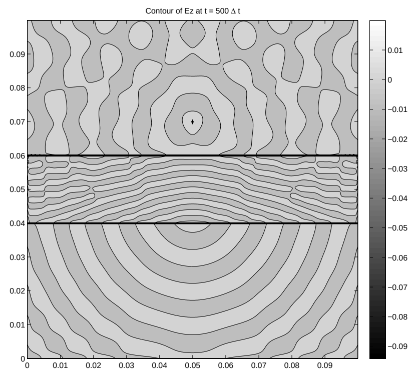

FIGURE 2. Contour of E_z at time $t = 500\Delta t$ from a point source above a lossy "unmatched" double-negative slab ($\epsilon_r = \mu_r \approx -3 - 0.002j$). Parameters are $\omega_{pe} = \omega_{pm} = 2\omega_0$, $\Gamma_e = \Gamma_m = 5.3 \times 10^{-4}\omega_0$, $\omega_0 = 2\pi f_0$ and $f_0 = 30G$.

by the EC-S-FDTD scheme. The electric field inside the metamaterial slab is approximately channeled into beams rather than being focused, as is showed in Figure 2.

Now, we carry out the simulation with an incident wave excitation in metamaterials. The center frequency of interest is chosen to be $f_0 = 30GHz$, corresponding to a free-space wavelength $\lambda_0 = 1.0cm$. The main scale of the computational domain is 600×200 with 10-cell PML layer in $x-$direction and $y-$direction respectively. With the Total-Field/Scatter-Field technology, we introduce the incident wave of the sinusoidal form and take the angular frequency $\omega = 2\pi f_0$ and the incident angle $\phi = \pi/9$. To illustrate the special character of DNG metamaterials, we give the classical propagation of oblique incidence plane wave in vacuum, in the regular dielectrics (i.e., double-positive (DPS) material) and in the DNG material, respectively (see Figure 3). All the results are obtained by our EC-S-FDTD scheme at the time $t = 840\Delta t$.

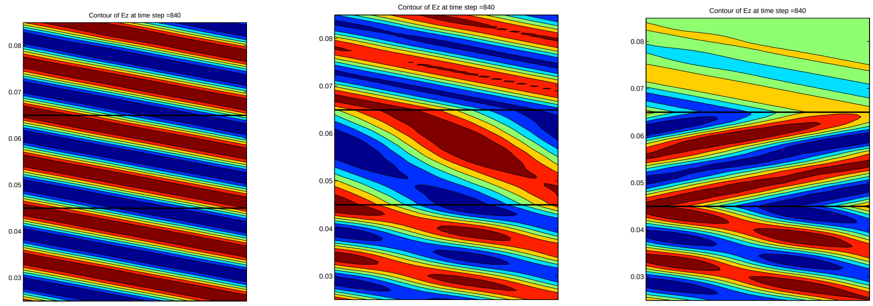

FIGURE 3. Contours of E_z from the interaction of a sinusoidal wave that is incident at an angle of 20° in vacuum (left), interaction with a DPS slab with the positive index of refraction $n = \frac{1}{2}$ (middle), and interaction with a DNG slab with the negative index of refraction $n = -1$(right).

Figure 3 (left) shows the distribution of E_z in vacuum without the existence of the DNG slab, which is of no deformation in the process of the wave propagation. The propagation of the wave in a DPS metamaterial with $\omega_{pe} = \omega_{pm} = \sqrt{2}\omega_0/2$, which leads to the index of refraction $n = \frac{1}{2}$, and $\Gamma_e = \Gamma_m = 0$ as shown in Figure 3 (middle). Since the index of refraction of this medium is less than that in vacuum, it is occurred that the refraction wave deviates more from the normal compared with the incident wave. Numerical results in Figure 3 (right) display the propagation of the wave in metamaterial with $\omega_{pe} = \omega_{pm} = \sqrt{2}\omega_0$, which leads to the index of refraction $n = -1$, and $\Gamma_e = \Gamma_m = 3.75 \times 10^{-4}\omega_{pm}$. A negative angle of refraction opposite to the angle of incidence is observed, which agrees with the physical character of the DNG metamaterial. Moreover, from these three figures in Figure 3, we can find the differences of E_z values which are caused by the different propagating speeds of the waves in different media. In vacuum, the wave propagates at the speed of $c = 3 \times 10^8$, while, in the other two media, the speeds of the waves are both smaller than that in vacuum and are relative to the parameters of the special metamaterial and the angular frequency of the incident waves.

Example 3. The problem in zero-index media. In this example, we further carry out the simulation of electromagnetic waves in zero-index Drude medium slabs, in which the permittivity and permeability are both near zero (and therefore the refractive index) at certain frequencies for applications such as delay lines, phase shifters, couplers and compact resonators.

We employ the scale of the slab as $d = 1.2\lambda_0$, $L = 10\lambda_0$, and choose $\omega_{pe} = \omega_{pm} = \omega_0$ and $\Gamma_e = \Gamma_m = 1.0 \times 10^{-5}\omega_0$ for the Drude model, leading to $\epsilon_r = \mu_r \approx 0.0 - 1.0 \times 10^{-5}j$ and we also take 40-cell PML layer to truncate the computational domain. Then, the line source is located at the center of the zero-index slab, normal to the $x-y$ plane. Figure 4 shows the contour of electric field intensity, where $C_N = 5$ is chosen in computation by the EC-S-FDTD scheme. It implies that the field radiated from the center of the zero-index slab propagates away orthogonally to the face of the slab. In fact, from Snell's law we know that the transmitted waves will have a transmitted angle of zero for any angle of incidence when the index of the incident medium is zero. The cylindrical wave generated by the line source will thus be converted into a wave with a planar wave front as the wave emerges from the matched zero-index slab. Moreover, as the wave propagates from the source outward through the matched zero-index slab, the constant electric field behaviour is being established within the slab. We can see from Figure 4 that the the electric field is constant within the whole slab, as expected for a matched zero-index medium.

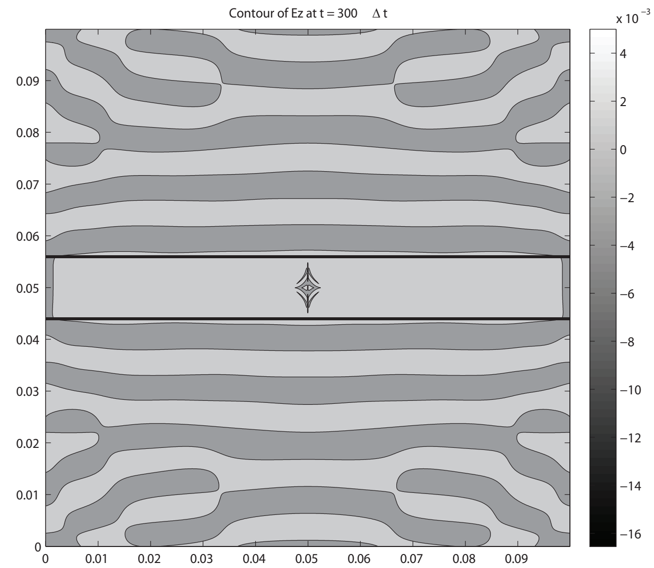

FIGURE 4. Contours of E_z from the line source located λ_0 above the front side of the zero-index slab ($\epsilon_r = \mu_r = 0.0 - 1.0 \times 10^{-5} j$) with thickness $d = 0.6\lambda_0$, $C_N = 5$, $\omega_0 = 2\pi f_0$ and $f_0 = 30G$ at $t = 300\Delta t$.

7. Conclusion

In this paper, we studied energy-conserved numerical computations of the Maxwell's equations in metamaterials. We first derived out a new energy conservation identity for Maxwell's equations in metamaterials. Then, a new energy-conserved S-FDTD scheme (EC-S-FDTD) is developed. We proved that the scheme satisfies the energy-conserved identity in the discrete form. We also analyzed the stability and the convergence of the scheme. In the part of numerical experiments, we first showed numerically the energy conservation and the accuracy of the scheme, which confirm to our theoretical results. Then, we simulated the propagation of electromagnetic waves in the DNG and DPS metamaterials and in the medium with a zero index of refraction. Physical phenomenna of electromagnetic waves in metamaterials were numerically observed and analyzed.

References

[1] F. Bilotti, and L. Sevgi, Metamaterials: definitions, properties, applications, and FDTD-Based modeling and simulation. Int. J. RF Microw. C. E., 22 (2012), 422-438.

[2] W. Chen, X. Li and D. Liang, Energy-conserved splitting FDTD methods for Maxwell's equations, Numer. Math., 108 (2008), 445-485.

[3] S. A. Cummer, Dynamics of causal beam refraction in negative refractive index materials. Appl. Phys. Lett., 82 (2003), 2008-2010.

[4] G. V. Eleftheriades and K. G. Balmain, Negative-Refraction Metamaterials: Fundamental Principles and Applications. Wiley: New York, 2005.

[5] N. Engheta, and R. W. Ziolkowski, A positive future for double-negative metamaterials. IEEE Trans. Microw. Theory Techn., 53 (2005), 1535-1556.

[6] N. Engheta, and R. W. Ziolkowski, Eds, In Metamaterials: Physics and engineering explorations. Wiley: New York, 2006.

[7] L. Gao, B. Zhang and D. Liang, The splitting-difference time-domain methods for Maxwell's equations in two dimensions, J. Comput. Appl. Math., 205 (2007), 207-230.

[8] S. G. Garcia, T. W. Lee, and S. C. Hagness, On the accuracy of the ADI-FDTD method. IEEE Antennas Wireless Compon. Lett., 13 (2002), 31-34.

[9] A. J. Holden, Towards some real applications for negative materials. Photonic and Nanostruct. Fundam. Appl., 3 (2005), 96-99.

[10] Y. Huang, J. Li, W. Yang, and Shuyu Sun, Superconvergence of mixed finite element approximations to 3-D Maxwell's equations in metamaterials. J. Comput. Phys. 230, No 22 (2011) 8275-8289

[11] Y. Huang, J. Li and W. Yang, Interior penalty DG methods for Maxwell's equations in dispersive media, J. Comput. Phys. 230, No 12 (2011) 4559-4570.

[12] S. Ju and H. Kim, A study of the numerical dispersion relation for the 2-D ADI-FDTD method. IEEE Microw. Wireless Compon. Lett., 13 (2003), 405-407.

[13] J. Li, Development of discontinuous Galerkin methods for Maxwell's equations in metamaterials and perfectly matched layers. J. Comput. Appl. Math., 209 (2011), 950-961.

[14] J. Li, Error analysis of fully discrete mixed finite element schemes for 3-D Maxwell's equations in dispersive media, Comput. Methods Appl. Mech. Engrg. 196 (2007) 3081- 3094.

[15] J. Li, Finite element study of the Lorentz model in metamaterials, Comput. Methods Appl. Mech. Engrg. 200 (2011) 626-637.

[16] J. Li, Optimal L^2 error estimates for the interior penalty DG method for Maxwell's equations in cold plasma. Commun. Comput. Phys. 11, No 2 (2012) 319-334.

[17] J. Li and Y. Huang, Mathematical simulation of cloaking metamaterial structures, Adv. Appl. Math. Mech., 4 (2012) 93-101.

[18] J. Li, Y. Huang and Y. Lin, Developing Finite Element Methods for Maxwell's Equations in a Cole-Cole Dispersive Medium. SIAM J. Sci. Comput., 33 (2011), 3153-3174.

[19] J. Li, Jiajia Wang Waters and R. A. Machorro, An implicit leap-frog discontinuous Galerkin method for the time-domain Maxwell's equations in metamaterials. Comput. Methods Appl. Mech. Engrg. 223/224 (2012) 43-54.

[20] J. Li and A. Wood, Finite element analysis for wave propagation in double negative metamaterials. J. Sci. Comput., 32 (2007), 263-286.

[21] F. Martin, Special issue on Microwave metamaterials: Theory, fabrication and applications. EuMA Proc 2, 2006.

[22] T. Namiki, A new FDTD algorithm based on alternating-direction implicit method. IEEE Trans. Microw. Theory Tech., 47 (1999), 2003-2007.

[23] V. E. Nascimento, K. Y. Jung, etc., A study on unconditionally stable FDTD methods for the modeling of metamaterials. J. Lightw. Technol., 27 (2009), 4241-4249.

[24] J. B. Pendry, Negative refraction makes a perfect lens. Phys. Rev. Lett., 85 (2000), 3966-3969.

[25] A. Shelby, D. R. Smith and S. Schultz, Experimental verification of a negative index of refraction. Science, 292 (2001), 489-491.

[26] D. R. Smith, W. J. Padilla and D. C. Vier, Nemat-Nasser, S. C., and Schultz, S., Composite medium with simultaneously negative permeability and permittivity. Phys. Rev. Lett., 84 (2000), 4184-4187.

[27] V. G. Veselago, The electrodynamics of substances with simultaneously negative values of ϵ and μ. Sov. Phys. Usp., 47 (1968), 509-514.

[28] V. Veselago, L. Braginsky, V. Shklover and C. Hafner, Negative refractive index materials. J. Comput. Theor., 3 (2006).

[29] F. Zheng, Z. Chen and J. Zhang, A finite-difference time-domain method without the Courant stability conditions. IEEE Microw. Guided Wave Lett., 9 (1999), 441-443.

[30] R. W. Ziolkowski, Wave propagation in media having negative permittivity and permeability. Phys. Rev. E., 64 (2001), 1-15.

[31] R. W. Ziolkowski, Design, fabrication, and testing of double negative metamaterials. IEEE Trans. Antennas Propag., 51 (2003), 1516-1529.

[32] R. W. Ziolkowski, Pulsed and CW Gaussian beam interactions with double negative metamaterial slabs. Opt. Exp., 11 (2003), 662-681.

The School of Mathematics, Shandong University, Jinan, Shandong, 250100, China
E-mail: `wanshanli@mail.sdu.edu.cn`

Department of Mathematics and Statistics, York University, Toronto, Ontario, M3J 1P3, Canada and The School of Mathematics, Shandong University, Jinan, Shandong, 250100, China
E-mail: `dliang@mathstat.yorku.ca`

Department of Applied Mathematics, The Hong Kong Polytechnic University, Kowloon, Hong Kong, P.R. China and Department of Mathematical and Statistical Sciences, University of Alberta, Edmonton, Alberta T6G 2G1, Canada
E-mail: `malin@polyu.edu.hk and yanlin@ualberat.ca`